Correlation between Maximum Temperature Increase and Peak SAR with Different Averaging Schemes and Masses

Akimasa Hirata, *Member, IEEE*, Masaki Fujimoto, Takayuki Asano, Jianqing Wang, *Member, IEEE*, Osamu Fujiwara, *Member, IEEE,* and Toshiyuki Shiozawa, *Fellow, IEEE*

***Abstract*— This paper investigates the correlation between maximum temperature increases and peak spatial-average SARs calculated by different averaging schemes and masses. For evaluating the effect of mass on the correlation properly, a 3-D Green's function is presented. From our computational investigation, no best averaging mass for peak spatial-average SAR exist from the aspect of the correlation with maximum temperature increase. This is attributed to the frequency dependent penetration depth of EM waves. Maximum temperature increase in the head including the pinna is reasonably correlated with peak spatial-average SARs for most averaging schemes and masses considered in this paper. Maximum temperature increase in the head only (excluding the pinna) is reasonably correlated with peak 10-g SARs for the averaging schemes considered in this paper. The rationale for this result is explained using the Green's function. The point to be stressed here is that the slope correlating them is largely dependent on the averaging scheme and mass. Additionally, good agreement is observed in the slopes obtained by using two head models, which have been developed at Osaka University and Nagoya Institute of Technology. However, weak correlation is observed for the brain, which is caused by the difference of the positions where peak SAR and maximum temperature increase appear. The 95th percentile values of the slope correlating maximum temperature increases in the head or brain and peak spatial-average SAR are quantified for different averaging schemes and masses.**

***Index Terms*— temperature increase, averaging schemes, SAR, dipole antenna, safety guidelines, possible health hazard, Green's function**

I. Introduction

In recent years, there has been increasing public concern about the health implication of electromagnetic (EM) wave exposure with the use of mobile telephones (e.g., see [1]). For this reason, public organizations throughout the world have established safety guidelines for EM wave absorption [2]–[5]. For RF near field exposures, these guidelines are based on peak spatial-average SAR (specific absorption rate) for any 1 or 10 g of body tissue. Incidentally, note that a different averaging scheme is used for each guideline. The temperature increase in the human body is one of the dominant factors due to microwave heating. A temperature increase of 4.5 [°C] in the brain has been noted to be an allowable limit which does not lead to any physiological damage (for exposures of more than 30 minutes) [6]. Additionally, the threshold temperature of the pricking pain in skin is 45 °C, corresponding the temperature increase of 10-15 °C [7]. It has been also reported that a temperature increase in the rabbit hypothalamus of 0.2 °C – 0.3 °C leads to altered thermoregulatory behavior [8]. It should be noted that diurnal variation of body core temperature is 0.2 °C – 0.3 °C [9], or comparable to the above threshold. The same group concluded that the humans demonstrate superior thermoregulatory ability against microwave exposures over other animals [10].

In view of these circumstances, the temperature increase in the anatomically based human head model for exposure to EM waves from handset antennas has been calculated [11]–[17]. In these papers, different averaging schemes and/or masses are used for calculating peak spatial-average SAR. One of the main reasons for this difference is that guidelines or standards define/suggest their unique averaging masses and shapes for peak SAR calculation. For example, SAR is averaged over 10 g of contiguous tissue in the ICNIRP guideline [4], while it is averaged over 10 g of tissues in the shape of a cube with a detailed regulation in the IEEE C95.3-2002 [18]. Note that 1 g has been used instead of 10 g until recently [2]. It is noteworthy that the effect of averaging procedure on peak SAR has been discussed analytically and then it was shown to be up to 20% or more at 900 MHz and 1800 MHz [19]. In the previous papers [11]–[17], different anatomically-based head models have also been used. This makes further difficulty to compare a maximum temperature increase at the limit of peak spatial-average SAR. In order to discuss this problem thoroughly, it is essential to evaluate the correlation between peak SAR and maximum temperature increase for different masses and averaging schemes. Then, this evaluation should be conducted for different head models.

In this paper, the maximum temperature increases in the head and brain are presented for different SAR averaging schemes, which are determined on the basis of the ICNIRP and IEEE guidelines. It should be noted that there are three major factors which affect the correlation between peak SAR and maximum temperature increase. One is the number of tissues taken into account. The second is the shape of averaging volume or not. The third difference is whether the pinnae are included in the averaging volume. In order to clarify these effects on the correlation, four averaging schemes are consid-

This work was partially supported by Grant-in-Aid for Young Scientist (B), The Ministry of Education, Culture, Sports, Science and Technology, Japan. A. Hirata, Asano, J. Wang and O. Fujiwara are with the Department of Electrical and Computer Engineering, Nagoya Institute of Technology, Nagoya 466-8555, Japan. M. Fujimoto is with Department of Communication Engineering, Osaka University, Yamada-oka 2-1, Suita-shi, Osaka 565-0871, Japan. T. Shiozawa is with Department of Electronics and Information Engineering, Chubu University, Aichi 487-8501, Japan. e-mail: ahirata@nitech.ac.jp

ered. The averaging masses of 1 g and 10 g are considered. For discussing the effect of mass, 3-D Green's function is introduced, and then specified for typical thermal constants of human tissues. Finally, for the head models developed at the Osaka University and Nagoya Institute of Technology (NIT), the maximum temperature increases in the head and brain are quantified and compared for these averaging schemes and masses. For our preliminary work, refer to [20].

II. Method and Model for the Analysis

A. Human Head Model

Two head models for the adult are considered: one has been developed at Nagoya Institute of Technology (NIT) [21] and the other at Osaka University [22]. These models are comprised of 17 and 18 tissues, respectively: bone (skull), muscle, skin, fat, white matter, grey matter, cerebellum, blood, and eye tissues, dura and C.S.F. For each model, unpressed and pressed ears are considered. The thicknesses of unpressed and pressed ears are 18 mm and 6 mm for the adult model of Osaka Univ., and 22 mm and 8 mm for the NIT adult model. The masses of the pinna are 8.7 g and 5.7 g for unpressed and pressed ear of the Osaka Univ. model. They are 9.8 g and 6.0 g for the NIT model.

B. Finite-Difference Time-Domain (FDTD) Method

The FDTD method is used for investigating the interaction between the human head model and a dipole antenna. In order to incorporate the inhomogeneous head model into the FDTD scheme, the dielectric properties of the tissues are required. They are determined by using the 4-Cole-Cole extrapolation [23]. For geometries in which wave-object interaction proceeds in the open region, the computational space has to be truncated by absorbing boundaries. In this paper, an 8-layered PML with a parabolic profile is adopted as the absorbing boundary.

As a wave source, a dipole antenna is considered. The diameter of the dipole antenna is fixed to 1.0 mm, while the length takes values of 160, 92, 72, 64, and 54 mm for 900 MHz, 1.5 GHz, 1.9 GHz, 2.1 GHz and 2.45 GHz, respectively. The output power of the antenna is 1.0 W. A continuous wave is injected to the antenna.

C. SAR Calculation

As mentioned above, a continuous wave is injected to the dipole antenna. In realistic environment, modulated waves are used. It should be noted that the peak-spatial SAR is defined as further averaging over a specific time period (e.g., 6 min. in [4]). Thus, the simplification of waveforms does not affect as far as discussing thermal elevation.

SAR is given by the following equation:

$$SAR = \frac{\sigma}{\rho}|\mathbf{E}|^2 \tag{1}$$

where $\mathbf{E}$ is the root mean square electric-field, σ and ρ denoting the conductivity and mass density of the tissue. Specifically, this equation is reduced to the following equation for harmonically-varying fields.

$$SAR = \frac{\sigma}{2\rho}|\hat{E}|^2 \tag{2}$$

TABLE I
Difference of averaging schemes in the IEEE standard and ICNIRP guideline.

	No. of Tissues	Shape of Avg. Volume	Pinna
(I)	unlimited	cube	excluded
(II)	1	contiguous	included
(III)	unlimited	cube	included
(IV)	unlimited	contiguous	included

where $\hat{E}$ is the peack value of the electric-field components.

For calculating peak spatial-average SAR, four schemes are considered in this paper. The first two schemes are based on the description in the IEEE standard C95.3-2002 [18] and the ICNIRP guideline [4]. These averaging schemes are defined as (I) and (II). There are three differences between these schemes: the number of tissues allowed in the averaging process, the shape of the averaging volume, and the pinna is included in the averaging volume or not. In the scheme (I), the shape of averaging volume is a cube, and different tissues are allowed. The averaging scheme is not defined clearly in (II); any 10 g of contiguous tissue. Then, we define a scheme, taking into account the description in the ICNIRP guideline [4]. First, voxel-SARs are sorted in the descending orders till the total mass of voxels becomes a specific mass (e.g., 10 g). The sorted voxels are divided into some groups in the following manner. One group is defined as a cluster of voxels, in which voxels are adjacent to each other. In the descending order, a specific voxel is judged whether its sides touch existent groups. If the voxel touches no group, a new group is assigned to the voxel. If it touches one of either group, the voxel belongs to the group. When the voxel touches different groups, these groups and the voxel are reclassified as a new group. This process is carried out for all the cells sorted in the above process. Finally, all groups are connected by choosing the shortest paths. As an averaging tissue, skin is chosen since it exists around the surface of the head.

In order to evaluate the differences of (I) and (II) on the correlation properly, additional two averaging schemes are introduced. Firstly, the SAR in the pinna is included in the averaging volume, while the remaining is identical to that of (I). This is defined as (III). The other scheme is based on (II), while any number of tissues is allowed in the averaging process. This is defined as (IV). The differences between these schemes are summarized in Table I.

D. Temperature Increase Calculation

The temperature in the human body is calculated by solving the bioheat equation. The SAR calculated by the FDTD method is used as the heat source. The bioheat equation [24], which takes into account the heat exchange mechanisms such as heat conduction, blood flow, and EM heating, is represented by the following equation:

$$C(\mathbf{r})\rho(\mathbf{r})\frac{dT(\mathbf{r},t)}{dt} = \nabla\cdot(K(\mathbf{r})\nabla T(\mathbf{r},t)) + \rho(\mathbf{r})(\mathrm{SAR}(\mathbf{r})) + Q(\mathbf{r}) - B(\mathbf{r})(T(\mathbf{r},t) - T_B) \tag{3}$$

where T is the temperature of the tissue, T the temperature of the blood, K the thermal conductivity of the tissue, C the specific heat of the tissue, Q metabolic heat generation, and B the term associated with blood flow. The temperature increase due to the antennas is assumed to be so small that it cannot activate the thermoregulatory response: the increase of local blood flow, the activation of sweating mechanism, and so forth. Thus, this effect is neglected in our discussion. The boundary condition for Eq. (3) is given by

$$H \cdot (T_s(\mathbf{r}) - T_e) = -K(\mathbf{r}) \frac{\partial T(\mathbf{r})}{\partial n} \tag{4}$$

where H, T_s, and T_e denote, respectively, the heat transfer coefficient, the surface temperature of the tissue, and the temperature of the air. The finite-difference expressions for Eqs. (3) and (4) are given in [12], [13]. Note that this paper does not treat the temperature increase due to the presence of handset terminal. Detailed discussion on this subject can be found in [25].

The temperature increase in the human model due to EM waves get saturated or becomes maximum at the thermally steady state. For this reason, the temperature increase at the thermally steady state is considered in this paper, corresponding to the worst case estimation. Eqs. (3) and (4) are reduced to the following equations at the thermally steady state:

$$\{\nabla \cdot (K(\mathbf{r})\nabla) - B(\mathbf{r})\}\delta T(\mathbf{r}) = -\rho(\mathbf{r})\mathrm{SAR}(\mathbf{r}) \tag{5}$$

$$\left(H + K(\mathbf{r})\frac{\partial}{\partial n}\right)\delta T(\mathbf{r}) = 0 \tag{6}$$

where $\delta T(\mathbf{r})$ is the temperature increase of tissue. Eq. (5) is a linear differential equation subject to the boundary condition (6).

Th equation (5) with the boundary condition (6) means that the temperature increase and SAR distributions are not identical. However, the temperature increase is linear in terms of the output power of the antenna, or the SAR amplitude at the thermally steady state. Note that it takes 30 minutes or more before the temperature increase gets saturated. It is also noteworthy that Q and C do not affect the temperature increase at the thermally steady state. Let us consider this problem on the basis of a Green's function. Note that the Green's function corresponding to (5) was firstly applied to the bioheat equation in [28]. Green's function satisfies the following equations:

$$L(\mathbf{r})G(\mathbf{r};\mathbf{r_i}) = -\delta(\mathbf{r} - \mathbf{r_i}) \tag{7}$$

$$L(\mathbf{r}) = \nabla \cdot (K(\mathbf{r})\nabla) - B(\mathbf{r}) \tag{8}$$

where $G(\mathbf{r};\mathbf{r_i}))$ is a Green's function associated with the differential operator L. The Green's function is dependent on the blood flow and heat conductivity, together with the heat transfer coefficient corresponding to air temperature (See Eq. (4)).

The temperature increase at a particular position is given in the discretized form as:

$$\delta T(\mathbf{r}) = \sum_i \rho(\mathbf{r_i}) SAR(\mathbf{r_i}) G(\mathbf{r};\mathbf{r_i}). \tag{9}$$

The Green's function for the bioheat equation will be evaluated later.

TABLE II
THERMAL PROPERTIES AND MASS DENSITIES OF TISSUES IN THE HUMAN HEAD.

Tissues	C [J/kg· °C]	K [W/m· °C]	B [W/m^3·°C]	ρ [kg/m^3]
Skin	3500	0.42	9100	1125
Muscle	3600	0.50	2700	10447
Bone	1300	0.40	1000	1700
Blood	3900	0.49	0	1058
Fat	2500	0.25	520	916
Grey Matter	3700	0.57	35000	1038
White Matter	3600	0.50	35000	1038
Cerebellum	4200	0.58	35000	1038
Humor	4000	0.60	0	1009
Lens	3000	0.40	0	1053
Sclera/Cornea	4200	0.58	0	1026
C.S.F.	4000	0.60	0	1007
Tongue	3300	0.42	13000	1047
Brain Dura	3600	0.50	2700	1125

E. Correlation between Peak SAR and Maximum Temperature Increase

We have demonstrated that maximum temperature increases in the head and brain are estimated linearly with peak spatial-average SARs in the corresponding regions [17]. Let us review the rationale for this result briefly. At the *thermally steady state*, the temperature increase is linear in terms of SAR. The SAR is proportional to the output power of wave sources. Thus, it could be appropriate to express maximum temperature increase approximately as:

$$\hat{T} = a \cdot \mathrm{SAR}_{ave} \tag{10}$$

where $\mathrm{SAR}_{ave}, \hat{T}$, and a denote, respectively, peak spatial-average SAR, the maximum temperature increase estimated by a regression line, which is determined by the method of least squares, and the slope of the regression line with the unit of °C · kg/W. The coefficient of determination, r^2, is used for evaluating the validity of the regression line [26], [27]. The closer to unity r^2 is, the better the correlation is. Note that the intercept of the regression line is set to zero since no temperature increase is induced without EM power absorption. A main reason why peak spatial-average SAR and maximum temperature increase are not fully proportional to each other is the difference between the SAR and temperature increase distributions, which are caused by the heat diffusion. Then, we pay attention to a one-voxel peak value for the temperature increase, while we note a peak value averaged over a specific mass for the SAR.

III. COMPUTATIONAL RESULTS

A. Green's Function of Bioheat Equation

This section presents Green's functions in order to give some insight into temperature increase in human tissues due to the application of heat source. Green's function indicates the thermal diffusion length under the application of a point heat source with unit strength, which roughly provides the volume where heat can diffuse. It is noteworthy that we have investigated 1-D Green's function for a modified bioheat equation in [29]. For obtaining Green's functions, the FD method is

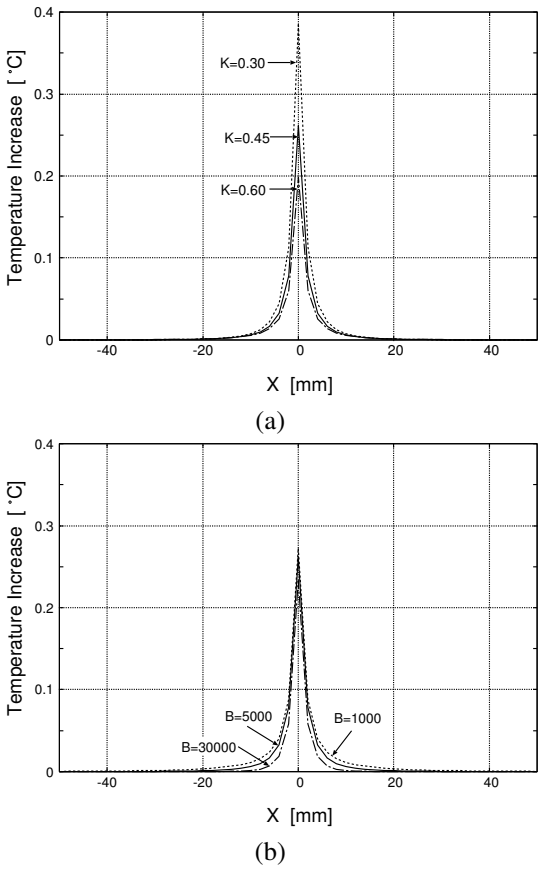

Fig. 1. Green's function for a point heat source given at the center of the cube (the side length 200 mm): Effects of (a) different heat conductivity (with B = 5000 W/m^3·°C) and (b) different term associated with blood flow (with K = 0.45 W/m· °C). $y = z = 0$.

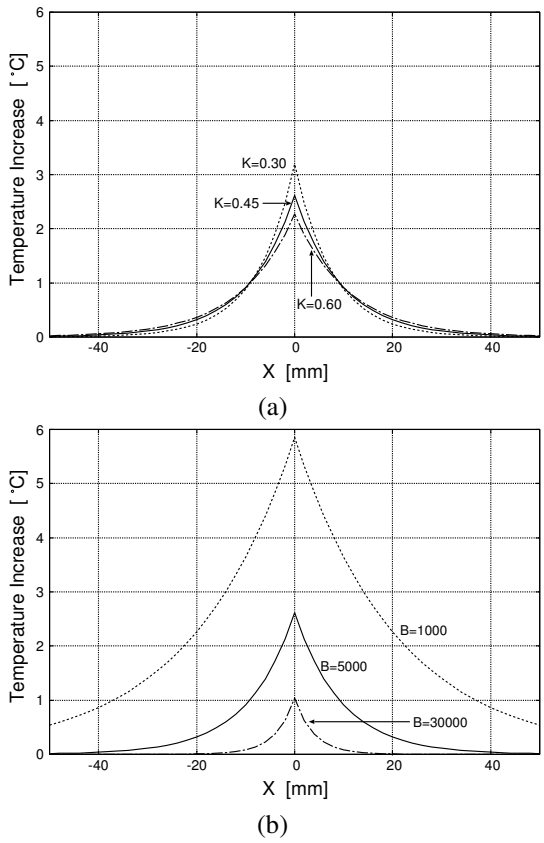

Fig. 2. Green's function for plane heat source given at the $y - z$ plane of the cube (200 mm): Effect of (a) different heat conductivity (with B = 5000 W/m^3·°C) and (b) different term associated with blood flow (with K = 0.45 W/m· °C). $y = z = 0$.

used for simplicity as is used for solving conventional bioheat equation [12], [13]. The cell size is set to 2 mm. Thermal diffusion length is defined as the length where the amplitude of heat decreases to ($1/e$). However, in this paper, this is defined as the length where the amplitude decreases to 5 %, since the value is comparable to the FD cell length.

For proper estimation of each effect on Green's function, one of the heat conductivity or blood flow rate is changed with the other parameter fixed. A point heat source with 1mW is given at the center cell of the cube with its side length of 200 mm. Figs. 1 (a) and (b) illustrate the effect of heat conductivity and blood flow rate on Green's function, respectively ($y = z = 0$). The origin of the coordinate corresponds to the center cell of the cube.

The term associated with blood flow is fixed to 5000 W/m^3·°C in 1 (a) and the heat conductivity is set to 0.45 W/m· °C) in 1 (b). From Fig. 1 (a), the amplitude of Green's function is affected by the heat conductivity by a factor of two. However, the thermal diffusion length is marginally affected by the heat conductivity: 6.55 mm for 0.30 W/m· °C, 7.05 mm for 0.45 W/m· °C, and 7.41 mm for 0.60 W/m· °C. From Fig. 1 (b), the thermal diffusion length is largely dependent on the blood flow rate: 8.91 mm for 1000 W/m^3·°C, 7.06 mm for 5,000 W/m^3·°C, and 5.19 mm for 30,000 W/m^3·°C. It should be noted that the peak amplitude at the heat source or the origin is almost independent on the blood flow.

In order to further investigate fundamental characteristics of heat diffusion in human tissues, heat sources are given on the $y - z$ plane uniformly (x=0 mm), almost corresponding to a 1-D case. As seen from Fig. 2, blood flow of human tissues is more dominant than that of heat conductivity for the temperature increase in a 1-D heat source, unlike for the case of a point source. This can be interpreted from Eq.(9), which states that the temperature increase is given by the superposition of green's function multiplied by heat potential (ρSAR).

Let us discuss the temperature increase due to RF near-field exposure, which is our main interest. The above Green's function suggested that the most dominant factor was the distance where heat can diffuse in a 3-D case. Main tissues around the surface of the human head are skin, fat, muscle, glands, when excluding the pinnae. The term associated with the blood flow B is in the range of 1,000 and 10,000 W/m^3·°C (See Table II). Then, roughly speaking, a distance where heat can diffuse is up to 2-6 cm as seen from Fig. 2. The EM waves decrease exponentially from the surface of human tissue. For muscle, the penetration depth of EM waves is around 12 mm at 2 GHz. As can be seen from Eq. (9), SAR distribution and the Green's function determine the temperature increase. This implies that the volume or mass required for properly estimating maximum temperature increase is dependent on

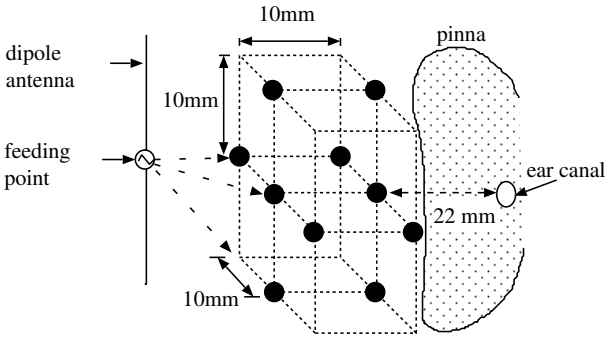

Fig. 3. The positions for the feeding point of the dipole antenna relative to the auricle. The distance between the original feeding point and ear canal is 22 mm.

the frequency of the EM waves, i.e., no best mass exists for correlating the SAR and temperature increase over the whole frequency band considered in this paper. Namely, an appropriate averaging volume would become smaller at higher frequencies.

B. Correlation between Peak SAR and Maximum Temperature Increase in the Head

This subsection discusses the correlations between peak spatial-average SARs and maximum temperature increase due to a dipole antenna. The following total of 400 situations is considered, and then the results are processed statistically:

- Two head models: adult models developed at NIT and Osaka Univ.;
- the head models with pressed or unpressed ear;
- five frequencies: 900 MHz, 1.5 GHz, 1.9 GHz, 2.1 GHz, and 2.45 GHz;
- two polarizations: the horizontal and vertical polarizations;
- ten feeding points (see Fig. 3).

The slope of the regression line (a) and the coefficient of determination (r^2) are compared for the models of Osaka Univ. and NIT. Note that no attention is paid to the correlation between maximum temperature increase in the head with the pinna and the SAR calculated by (I). This is because good correlation is not observed when the positions where peak SAR and maximum temperature increase are not coincident [17]. Also note that comparison between our results and other groups, can be found in the same reference.

First, the effect of averaging shape for peak SAR on the correlation is discussed. Then, our attention is paid to the results for the schemes of (III) and (IV). When our attention is paid to maximum temperature increase in the head with the the pinna (see Table III (a)), the correlations are good for these averaging schemes. This is also true for different averaging masses. It should be noted that the slope of the regression line is largely affected by the SAR averaging mass and scheme. The difference in the slope of the regression line is at most 10% between these two models for the cases considered.

From Table III (b), maximum temperature increase in the head only (i.e., without the pinna) is reasonably correlated in terms of peak 10-g SARs. Even for peak 10-g SARs, the coefficients of determination is worse than those in Table III (a). This is because large SAR values appear in the pinna for most cases, while our attention is paid to maximum temperature increase in the head only. Then the conduction of heat evolved in the pinna is not negligible, while this is not taken into account in the peak SAR calculation.

TABLE III

CORRELATION BETWEEN PEAK SAR AND MAXIMUM TEMPERATURE INCREASE FOR DIFFERENT AVERAGING SCHEMES AND MASSES: MAXIMUM TEMPERATURE INCREASE IN (a) HEAD WITH THE PINNA AND (b) HEAD ONLY IS CONCERNED.

(a)

	Osaka Univ.		NIT	
	a	r^2	a	r^2
(II) ; 1 g	0.0573	0.982	0.0586	0.943
(II) ; 10 g	0.131	0.833	0.147	0.637
(III) ; 1 g	0.0705	0.833	0.0633	0.913
(III) ; 10 g	0.152	0.874	0.165	0.758
(IV) ; 1 g	0.0558	0.978	0.0561	0.935
(IV) ; 10 g	0.113	0.874	0.124	0.688

(b)

	Osaka Univ.		NIT	
	a	r^2	a	r^2
(I) ; 1 g	0.129	0.877	0.0907	0.833
(I) ; 10 g	0.227	0.887	0.187	0.734
(II) ; 1 g	0.0462	0.637	0.0344	0.181
(II) ; 10 g	0.109	0.772	0.0858	0.633
(III) ; 1 g	0.0631	0.368	0.0348	0.0472
(III) ; 10 g	0.133	0.674	0.106	0.516
(IV) ;1 g	0.0486	0.755	0.0345	0.354
(IV) ;10 g	0.104	0.834	0.0777	0.800

Next, we discuss the effect of number of tissues allowed in the averaging process on the correlation. Then, the results for the schemes of (II) and (IV) are compared in this discussion. For microwave exposures, large SAR appears around the surface of the body. The skin exists on the surface of the head and is contiguous. Then, the skin is chosen as an averaging tissue. When maximum temperature increase in the head with the pinna is considered, these averaging schemes are comparable. This is because the thickness of the pinna is at most 6 mm in our modeling. Namely, the skin is the dominant tissue in the pinna. Marginal difference is observed in the choice of averaging volumes. On the other hand, the correlation obtained by the scheme of (IV) is better than that of (II) for maximum temperature increase in the head only. This is because SAR is averaged for the skin tissue only, and thus averaging volume is distributed on the surface of the head widely. Peak SAR appears around the root of the pinna, i.e., around the edge of the averaging volume. Then, the positions of peak SAR and maximum temperature increase are not coincident with each other, leading to weak correlation.

Let us discuss the correlation between maximum temperature increase in the head only and peak SAR calculated by (I) and (III). When SAR is averaged for the head only (scheme (I)), correlations better than that for the head with the pinna (scheme (III)) are observed for both the averaging masses. This could be attributed again to the difference in the positions of maximum temperature increase and peak SAR.

For the four averaging schemes, peak 10-g SAR is a measure better than peak 1-g SAR, when we pay attention to maximum temperature increase in the head only (see Table III(b)). Particularly, the difference in the slope of the regression lines is marginal for the two head models. Let us discuss the rationale for this. As explained in Sec. II.D, the bioheat equation is reduced to a linear equation in terms of SAR at the thermal steady state. By virtue of the linearity, which is given in Eq. (9), the contribution of SAR in the averaging volume only to maximum temperature increase can be discussed quantitatively. Namely, the SAR outside the averaging volume is assumed as nonexistent in this fictitious discussion. The averaging scheme (I) is chosen as an example. As a feeding point, we consider the 'original position' in Fig. 1. At the frequency of 2.45 GHz, maximum temperature increase due to the SAR in the whole head was 1.44 °C. For SAR in the averaging volume only, temperature increases at the same position were 1.28 °C and 0.43 °C for the averaging masses of 10 g and 1 g; the contributions of SAR in the averaging volume are 88% and 29%, respectively. At the frequency of 900 MHz, these values are 0.39 °C and 0.15 °C, while the original temperature increase is 0.72 °C. These results suggest that the contribution of SAR in the surrounding region of averaging volume can be significant when 1 g is chosen as the averaging mass. In other words, the heat conduction from the surrounding region is not negligible for peak 1-g SAR.

Let us discuss the results of (I) in Table 1(b) again. The differences in the slope between the models of Osaka Univ. and NIT is 20% for the averaging mass of 10 g while 35% for 1 g. Main reasons for this could be the dimension and complexity of the pinna. The amount of EM deposition in the pinna is largely affected by these factors, leading to different amount of heat diffusion from there to a position where a maximum temperature increase appears. It is also noteworthy that we have investigated the correlation for the models of child, which were developed from these adult models. The slopes of regression lines in terms of peak 10-g SAR is less sensitive to different models than those for peak 1-g SAR [31]. This implies that the usage of 10-g averaging mass would result in the suppression of uncertainties in the correlation caused by heat conduction from the pinna and/or surrounding region due to larger averaging mass. Note also that the complexity of the pinna can change a surface area of the head, leading to a different amount of heat convection. This effect would be enhanced when the stair-casing model is used [30].

As far as the temperature increase in the head with the pinna is concerned, peak 1-g SAR is marginally better. Similar to the above discussion, the contribution of SAR in the averaging volume to maximum temperature increase is investigated by using the averaging scheme (III). At the frequency of 2.45 GHz, the contributions of SAR in the averaging volume to maximum temperature increase are 96% and 83% for the averaging masses of 10 g and 1 g. The point to be stressed is that the contribution of SAR in the averaging volume is large as compared with the case in the temperature increase in the head only. This is mainly caused by the shape of the pinna. Namely, the thickness of the pinna is small, and then the side length of the cube for averaging process becomes large. For example, the side length of the averaging volume is 14 mm for the 'original' feeding point defined in Fig. 1 at 900 MHz.

TABLE IV
EFFECT OF DIFFERENT AVERAGING SCHEME AND MASS ON THE CORRELATION OF PEAK SAR AND MAXIMUM TEMPERATURE INCREASE IN BRAIN.

	Osaka Univ.		NIT	
	a	r^2	a	r^2
(I) ; 1 g	0.0361	0.360	0.0315	0.002
(I) ; 10 g	0.0721	0.554	0.0667	0.384
(II) ; 1 g	0.0151	0	0.00891	0
(II) ; 10 g	0.0345	0.402	0.0263	0
(III) ; 1 g	0.0182	0	0.00961	0
(III) ; 10 g	0.0405	0.066	0.284	0.011
(IV) ; 1 g	0.0147	0.094	0.00851	0
(IV) ; 10 g	0.0311	0.491	0.0229	0.141

C. Correlation between Peak SAR and Maximum Temperature Increase in the Brain

Table IV lists the correlations between peak SAR and maximum temperature increase in the brain for both the head models. As compared with the correlation for maximum temperature increase in the head, the correlations are weak. The reason for this weak correlation would be the difference of the positions where peak SAR and maximum temperature increase in the brain appear. Namely, the majority of power absorption appears around the surface of the head, while we pay attention to a maximum temperature increase in the brain, which is located at the surface of the brain, corresponding to around 20 mm or more from the surface of the head. The averaging scheme (I) with the averaging mass of 10 g is reasonable to correlate peak SAR and maximum temperature increase as compared with the others. Using the averaging scheme (I), the frequency dependency of the slope of the regression line is shown in Fig. 4. Then, 40 cases are considered for each frequency (see Fig. 1). Note that good correlation (0.8 or better) is observed at each frequency. From Fig. 4, the frequency dependency of the slope of the regression line is observed. This is attributed to skin depth of EM waves. At the higher frequencies, an EM wave is absorbed around the surface of the head, resulting in smaller heat conduction to the brain than that at the lower frequencies. The point to be stressed is that the slope correlating peak SAR and maximum temperature increase in the brain is marginally dependent on head models, when peak 10-g SAR calculated by the scheme (I) is used. The reason for this marginal dependency could be almost identical to the discussion in Sec. 3.1, and thus omitted to avoid repetition.

D. Possible Maximum Temperature Increase in Head and Brain for Different SAR Averaging Schemes

This subsection discusses maximum temperature increases in the head with the pinna, the head only, and the brain. As a measure for comparison, the 95th percentile is used. As we consider 200 cases for each averaging scheme, this

corresponds to the 191st value in the ascending order. Note that maximum values of possible temperature increases are roughly estimated by the product of the SAR limit in the guidelines and this slope. It should be noted that the upper limit for near-field microwave exposures in public environments is 2.0 W/kg for 10 g of tissue [3], [4].

Table V shows the 95th percentile values of the slope correlating maximum temperature increases and peak spatial-average SARs. Comparing Tables III and V, similar trend is observed. Namely, the slopes for the two head models are small for specific averaging schemes. On the other hand, no clear difference between the two models is observed for 95th percentile slope of the brain, while their correlations were not good. This is attributed to the frequency dependency of the regression line as shown in the above section. Possible maximum temperature increase in the brain occurs at lower frequencies due to large skin depth of EM waves (see Fig. 4). At the same frequencies, good correlations were observed, getting comparable with the 95th value of the slope of the regression line. The point to be stressed is that 95th percentile values for the slope of the regression line are affected by the schemes and masses by a factor of 2–3.

TABLE V

95TH PERCENTILE VALUES OF THE SLOPE CORRELATING BETWEEN MAXIMUM TEMPERATURE INCREASES AND PEAK 1-G/10-G SAR: THE MAXIMUM TEMPERATURE INCREASES IN (a) HEAD WITH THE PINNA AND (b) HEAD ONLY AND (c) BRAIN ARE CONSIDERED.

(a)

	1 g		10 g	
	Osaka	NIT	Osaka	NIT
(II)	0.0637	0.0717	0.171	0.242
(III)	0.121	0.886	0.211	0.280
(IV)	0.0632	0.0705	0.141	0.208

(b)

	1 g		10 g	
	Osaka	NIT	Osaka	NIT
(I)	0.166	0.117	0.293	0.258
(II)	0.0615	0.0637	0.144	0.111
(III)	0.120	0.0854	0.207	0.161
(IV)	0.0611	0.0607	0.123	0.0951

(c)

	1 g		10 g	
	Osaka Univ.	NIT	Osaka Univ.	NIT
(I)	0.0621	0.0599	0.107	0.107
(II)	0.0259	0.0377	0.0488	0.0611
(III)	0.0485	0.0447	0.0785	0.0871
(IV)	0.0255	0.0372	0.0447	0.0505

IV. SUMMARY

This paper investigated the correlation between maximum temperature increase in the head and brain and peak spatial-average SAR calculated by different averaging schemes and masses. The rationale for this investigation was that the temperature increase may be one of the dominant factors which induce adverse physiological effects, although peak SAR is used as a measure for human protection. In previous papers, different anatomically-based head models are used for thermal dosimetry, together with different averaging masses and schemes. This was because each organization recommended its unique guideline/standard. In order to evaluate the effect of averaging masses and schemes, four averaging schemes and two masses were applied. Especially for investigating the effect of averaging mass on the SAR-temperature increase correlation, 3-D Green's function was introduced for typical thermal parameters of human tissues.

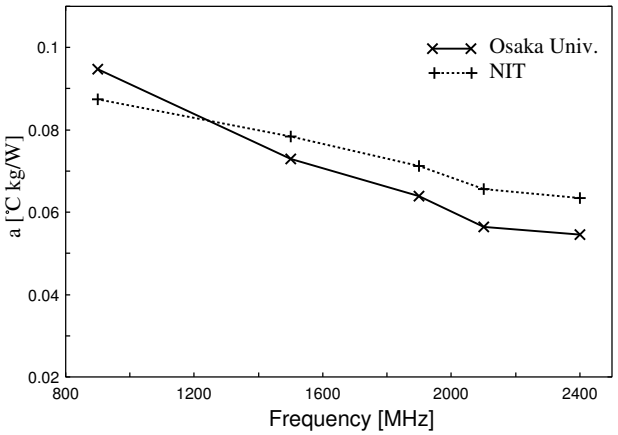

Fig. 4. Frequency dependency of the slope of regression line for maximum temperature increase in the brain.

Formulation in terms of Green's function did not suggest that the best averaging mass for peak SAR exist from the aspect of the correlation with maximum temperature increase, which is attributed to the frequency-dependent nature of EM wave absorption. From our computational investigation, together with statistical processing, it was found that maximum temperature increases in the head with pinna were well correlated with peak spatial-average SARs calculated for most averaging schemes and masses considered in this paper. However, the slope correlating them was largely dependent on the averaging schemes and masses. Note that the averaging schemes (II) and (IV) with the averaging mass of 1 g were reasonable for estimating average and 95th value of the slope of the regression line. For maximum temperature increase in the head only, averaging mass of 10 g was better than that of 1 g. Especially, the scheme (I) was the best, while no obvious difference is found. Then, the effect of averaging schemes on the correlation was marginal; the coefficient of determination was good for the cases considered in this paper. The reason for this result was explained using the thermal diffusion length in human tissues. In other words, heat diffusion from the pinna and surrounding region was found to be obvious using 1 g as an averaging mass.

The correlation for the brain was, however, dependent on the frequency of EM waves. This was caused by the skin depth of EM waves. Then, larger temperature increase in the brain was observed at lower frequencies. The point to be stressed here is that good agreement was observed in the slopes between two head models for maximum temperature increases in the head and brain. Furthermore, the 95th percentile values of the slope correlating maximum temperature increase and the SAR values were also quantified as a measure of the worst case. This quantification would be useful for comparing the temperature increase at different safety limits.

APPENDIX

According to the IEEE C95.3-2002, the pinna follows the limit for extremities. Namely, the limit of 4 W/kg is applied to the pinna. The point to be stressed here is that the temperature increase in the head excluding the pinna is affected by the SAR or EM deposition in the pinna. In other words, the SAR in the head only and that in the pinna cannot be considered separately from the aspect of temperature increases. Firstly, the correlation between peak SAR in the pinna and maximum temperature increase in the pinna are discussed for the averaging mass of 10 g. It should be noted that the masses of the pinna are less than 10 g for our models. Thus, the SAR is averaged over the whole pinna. The slope of correlating maximum temperature increase in the pinna and SAR averaged over the pinna are listed in Table VI. From this table, the slope of the regression line is marginally dependent on the ear condition, i.e., pressed and unpressed ears. The difference in the slope between two models are not large. It is noteworthy that this slope are comparable with the results of(III) and (IV) with the mass of 10 g in Table 1.

Next, the SAR averaged over the pinna (about 10 g) and peak SAR for the head only are calculated separately. Then, these values are compared with the limits of 4 W/kg and 2 W/kg, respectively. Comparing these SARs and the limits, the maximum temperature at the SAR limit is investigated. Possible maximum temperature increases for the SAR limits are listed in VII. Marginal difference is observed between these values and those calculated from Table V for the averaging scheme (I). It is worth commenting that temperature increases due to the average SAR in the pinna for the limit of 4 W/kg are larger than those due to the peak SAR in the head for the limit of 2 W/kg for the head models with unpressed ear.

TABLE VI
CORRELATION OF PEAK SAR AND MAXIMUM TEMPERATURE INCREASE IN THE PINNA.

	Osaka Univ.		NIT	
	a	r^2	a	r^2
Pressed Ear	0.157	0.864	0.164	0.846
Unpressed Ear	0.140	0.814	0.160	0.956
Both Ears	0.146	0.824	0.161	0.916

REFERENCES

[1] M. Burkhardt and N. Kuster, "Review of exposure assessment for hand-held mobile communications devices and antenna studies for optimized performance," (*Review of Radio Science 1996–1999* edited by W. R. Stone), Oxford Univ. Press, 1999 chap, 34.

[2] ANSI/IEEE C95.1-1992, Safety Levels with Respect to Human Exposure to Radio Frequency Electromagnetic Fields, 3 kHz to 300 GHz, New York: IEEE.

TABLE VII
POSSIBLE MAXIMUM TEMPERATURE INCREASES AT THE SAR VALUES PRESCRIBED IN THE IEEE GUIDELINES.

	Osaka Univ.	NIT
pinna	1.10	0.796
head only	0.524	0.484
brain	0.214	0.206

[3] "Radio-radiation protection guidelines for human exposure to electromagnetic fields," Telecommun. Technol. Council Ministry Posts Telecommun., Deliberation Rep. 89, Tokyo, Japan, 1997.

[4] International Commission on Non-Ionizing Radiation Protection (ICNIRP), "Guidelines for limiting exposure to time-varying electric, magnetic and electromagnetic fields (up to 300 GHz)," *Health Phys.*, vol.74, pp.494-522, 1998.

[5] IEEE C95.1-2005, Safety Levels with Respect to Human Exposure to Radio Frequency Electromagnetic Fields, 3 kHz to 300 GHz, New York: IEEE.

[6] A. C. Guyton and J. E. Hall, *Textbook of Medical Physiology*, Philadelphia, PA: W. B. Saunders, 1996.

[7] J. D. Hardy, H. G. Wolff, and H. Goodell, *Pain Sensations and Reactions,* Baltimore, MD: Williams &Wilkins, 1952, chap IV and X.

[8] E. R. Adair, B. W. Adams, and G. M. Akel, "Minimal changes in hypothalamic temperature accompany microwave-induced alteration of thermoregulatory behavior," *Bioelectromagnetics*, vol.5, pp.13–30, 1984.

[9] I. F. M. Marai, A. A. M. Habeeb, A. E. Gad, "Rabbits' productive, reproductive and physiological performance traits as affected by heat stress: a review," *Livestock Product. Sci.*, vol.78, pp.71-90, 2002.

[10] E. R. Adair and D. R. Black, "Thermoregulatory responses to RF energy absorption," *Bioelectromagnetics Supplement*,vol.6, pp.S17-S18, 2003.

[11] G. M. J. Van Leeuwen, J. J. W. Lagendijk, B. J. A. M. Van Leersum, A. P. M. Zwamborn, S. N. Hornsleth, and A. N. T. Kotte, "Calculation of change in brain temperatures due to exposure to a mobile phone," *Phys. Med. Biol.*, vol. 44, pp.2367-2379, 1999.

[12] J. Wang and O. Fujiwara, "FDTD computation of temperature rise in the human head for portable telephones," *IEEE Trans. Microwave Theory & Tech.,* vol.47, pp.1528-1534, 1999.

[13] P. Bernardi, M. Cavagnaro, S. Pisa, and E. Piuzzi, "Specific absorption rate and temperature increases in the head of a cellular-phone user," *IEEE Trans. Microwave Theory & Tech.,* vol.48, pp.1118-1126, 2000.

[14] P. Wainwright, "Thermal effects of radiation from cellular telephones," *Phys. Med. Biol.*, vol.45, pp.2363-2372, 2000.

[15] O. P. Gandhi, Q.-X. Li, and G. Kang, "Temperature rise for the human head for cellular telephones and for peak SARs prescribed in safety guidelines," *IEEE Trans. Microwave Theory & Tech.,* vol.49, no.9, pp.1607-1613, 2001.

[16] A. Hirata, M. Morita, and T. Shiozawa, "Temperature increase in the human head due to a dipole antenna at microwave frequencies," *IEEE Trans. Electromagnetic Compt.*, vol.45, no.1, pp.109-117, Feb. 2003.

[17] A. Hirata and T. Shiozawa, "Correlation of maximum temperature increase and peak SAR in the human head due to handset antennas," *IEEE Trans. Microwave Theory & Tech.*, vol.51, no.7, pp.1834-1841, July 2003.

[18] Annex E in IEEE C95.4-2005 Standard, New York: IEEE.

[19] N. Stevens and L. Martens, "Comparison of averaging procedures for SAR distributions at 900 and 1800 MHz," *IEEE Trans. Microwave Theory & Tech.*, vol.48, no.11, pp.2180–2184, 2000.

[20] A. Hirata, M. Fujimoto, J. Wang, O. Fujiwara, and T. Shiozawa, "Maximum temperature increases in the head and brain for SAR averaging schemes prescribed in safety guidelines," *IEEE Int'l Symp. Electromanget. Compat.*, vol.3, pp.801-804, Aug. 2005.

[21] J. Wang and O. Fujiwara, "Dosimetric evaluation of human head for portable telephones," *Electron. & Comm. Japan, Part I*, vol.85, pp.12-22, 2002.

[22] A. Hirata, S. Matsuyama, and T. Shiozawa, "Temperature rises in the human eye exposed to EM waves in the frequency range 0.6 – 6 GHz," *IEEE Trans. Electromagnetic Compt.*, vol.42, no.4, pp.386–393, Nov. 2000.

[23] C. Gabriel, "Compilation of the dielectric properties of body tissues at RF and microwave frequencies," *Final Technical Report Occupational and Environmental Health Directorate* AL/OE-TR-1996-0037 (Brooks Air Force Base, TX: RFR Division).

[24] H. H. Pennes, "Analysis of tissue and arterial blood temperature in resting forearm," *J. Appl. Physiol.*, Vol.1 pp.93–122, 1948.

[25] A. Ibrahiem, C. Dale, W. Tabbara, and J. Wiart, "Analysis of the temperature increase linked to the power induced by RF source," *Progress in Electromagnetic Res.*, vol.52, pp.23-46, 2005.

[26] L. Sachs, *Applied Statistics: A Handbook of Techniques: 2nd Ed.,* New York: Springer-Verlag, 1982.

[27] L. L. Lapin, *Statistics: Meaning & Method*, New York: Harcourt Brance Jovanovich, INC., 1975.

[28] Z-S. Deng and J. Liu, "Analytical study on bioheat transfer problems with spatial or transient heating on skin surface or inside biological bodies," *Trans. ASME J. Biomecha. Eng.*, vol.124, pp.638-649, 2002.

[29] A. Hirata, K. Yoshida, M. Fujimoto, J. Wang, and O. Fujiwara, "Correlation between temperature increase and spatial averaged SAR in the human head model due to dipole antenna," *Int'l Conf. Electromagnet. Compat.*, no.4A-3, Jul. 2005 (Phuket, Thailand).

[30] T. Samaras and N. Kuster, "Software tool for the calculation of temperature distributions induced by electromagnetic absorption," *Proc. of 4th European Bioelectromagnetics Assoc. Cong.*, p.91

[31] M. Fujimoto, A. Hirata, J. Wang, O. Fujiwara, and T. Shiozawa, " Inherent correlation of maximum temperature increase and peak SAR in child and adult head models due to a dipole antenna," to be published in *IEEE Trans. Electromagnet. Compat.*